PROCEEDINGS OF SPIE

SPIEDigitalLibrary.org/conference-proceedings-of-spie

Mirror module design of x-ray telescopes of eXTP mission

S. Basso, M. Civitani, G. Pareschi, G. Sironi, D. Spiga, et al.

S. Basso, M. Civitani, G. Pareschi, G. Sironi, D. Spiga, G. Tagliaferri, J. Wang, Y. Yang, Y. Xu, Y. Chen, L. Sheng, Y. Yan, P. Qiang, B. Zhao, "Mirror module design of x-ray telescopes of eXTP mission," Proc. SPIE 11119, Optics for EUV, X-Ray, and Gamma-Ray Astronomy IX, 1111904 (9 September 2019); doi: 10.1117/12.2530807

SPIE.

Event: SPIE Optical Engineering + Applications, 2019, San Diego, California, United States

Mirror module design of x-ray telescopes of eXTP mission

S. Basso[a], M. Civitani[a], G. Pareschi[a], G. Sironi[a], D. Spiga[a], G. Tagliaferri[a], J. Wang[b], Y. Yang[b], Y. Xu[b], Y. Chen[b], L. Sheng[c], Y. Yan[c], P. Qiang[c], B. Zhao[c]

[a]INAF-Brera Astronomical Observatory, Via E. Bianchi 46, 23807 Merate, Italy
[b]IHEP, Institute of High Energy Physics, 19B Yuquan Road, Shijingshan district, Beijing, 100049, China
[c]XIOPM, Xi'an Institute of Optics and Precision Mechanics, CAS, NO.17 Xinxi Road, Xi'an, Shaanxi, China

ABSTRACT

The eXTP (enhanced X-Ray Timing and Polarimetry) mission is a Chinese science space mission developed in collaboration with many international countries. Devoted to observations in the X-ray band, with imaging, spectroscopic, timing and polarimetry capabilities, is now entering phase B. The payload includes 9 Spectroscopic Focusing Array (SFA) and 4 Polarimetry Focusing Array (PFA) telescopes. The SFA telescopes, equipped with SDDs, have a spatial resolution of 1 arcmin, while the PFA telescopes, equipped with imaging gas pixel photoelectric polarimeters, have a spatial resolution of 30 arcsec. Both optics work in the 0.5-10 keV range with a focal length of 5.25 m and a field of view of 12 arcmin. The technology used for the optics production is Nickel electroforming from super-polished mandrels, like many previous successful X-ray missions. The reflecting coating is a double layer Au+C, which ensures optimal response at high and low energies. The PFA and SFA have the same optical design, in order to minimize the number of mandrels to be produced. In this paper, we present the optical design of these telescopes assisted with raytracing and a preliminary concept for the mechanical design supported by FEM simulation.

Keywords: eXTP, X-ray optic, Mirror module, polarimeter, X-ray telescope

1. INTRODUCTION

Optics made in electroformed Nickel have been a milestone for the X-ray telescopes. Many missions have extensively used this technology: BeppoSax, JetX/Swift, XMM/Newton, eROSITA, ART-XC and the oncoming IXPE. The latter will be the first mission equipped with a polarimeter. X-ray polarimetry is one of the main scientific goals of the eXTP[1] mission, which is equipped with 9 mirror modules dedicated to spectroscopy (SFA) and 4 mirror modules dedicated to the detection of polarized X-rays (PFA). An artistic representation of the mission is shown in Figure 1.

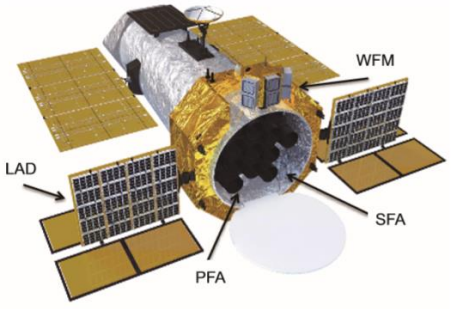

Figure 1 - Artistic view of the eXTP spacecraft (credit: Institute of High Energy Physics Chinese Academy of Sciences, Beijing, China). The science payload consists of four instruments: the focused SFA and PFA telescopes arrays, the large area instrument LAD, and the WFM to monitor a large fraction of the sky.

Optics for EUV, X-Ray, and Gamma-Ray Astronomy IX, edited by Stephen L. O'Dell, Giovanni Pareschi, Proc. of SPIE Vol. 11119, 1111904 · © 2019 SPIE · CCC code: 0277-786X/19/$21 · doi: 10.1117/12.2530807

The electroforming process for mirror shells manufacturing is a well mature technology developed and consolidated in the past two decades[2][3][4] in Italy by INAF/OAB (Brera Astronomical Observatory) in collaboration with Media-Lario Technologies, aimed at obtaining thin mirror shells (a few hundreds of microns) with an angular resolution in the range of 10-30 arcsec HEW (Half Energy Width) in the energy band of 0.5-40 keV. Moreover, using a similar approach based on the Ni electroforming replication, at NASA-Marshall Space Flight Center (MSFC) the thin mirror shells for the ART-XC instrument[5] aboard the Spectrum-Röntgen-Gamma mission have been produced and the shells for IXPE[6] polarimetric mission are being developed.
The main parameters for the X-ray telescope of the eXTP mission are summarized in Table 1.

Table 1 – Mirror Module main parameters of eXTP telescope

Item	*Requirement of SFA*	*Requirement of PFA*
Number of MMs*	9	4
Focal length	5.25 m	
Envelope (include mounting lugs)	≤ 600 mm in diameter	
Length of mirror shells	600 mm	
Effective area on axis per MM	≥820 cm² @ 2 keV, ≥550 cm² @ 6 keV	
Energy range	0.5~10 keV	
Field of view	12′	
Angular resolution	1′ (HPD)、3′ (W90)	30″ (goal 15″, HPD)
Mass budget mirror shells, mechanical structure to interface (auxiliary item excluded)	≤ 100 kg for each MM	
Working temperature	20±1℃	

In order to fulfil the requirements for the mass and the effective area, the choice of the thickness for the mirror shells is essential, taking into account also the required angular resolution and the engineering requirements for launch survival. In this respect, thinner mirror shells in general lead to poorer angular resolution for manufacturing reasons, and to a greater deformation under the environment loads. The ratio between the thickness and the mirror shell radius (t/r), considered as the driving parameter, is set to 0.00175. In general, this ratio remains constant throughout each mirror module from the inner to the outer radius. The t/r value for the other mission is shown in Table 2.

Table 2 – thickness/radius ratio for X-ray telescopes based on electroformed Nickel mirror shells.

mission	*t/r*	*Length (par+hyp)*	*HEW [arcsec]*	*n. spider*
Beppo-SAX[7]	~0.007	300	~50	2
Jet-X/Swift[8]	~0.007	600	~20	2
XMM/Newton[9]	~0.003	600	~15	1
eROSITA[10]	~0.003	300	~18	1
IXPE[11]	~0.002	600	~25	1

The t/r value for eXTP is similar to the value used for IXPE, even if the diameter for eXTP is bigger (435 mm w.r.t. 272 mm) and also similar to the value adopted in the prototypes developed for the NHXM studies[12]. Anyway, adopting such a low thickness, the mirror shell is intrinsically very flexible. Therefore, the use of one or two spiders for gluing the edges of the shells should be very carefully assessed. Possible problems related to the use of a single spider might reside in a too low resonance frequency, gluing failure, collision between mirror shells or permanent deformation at the time of launch. On the other hand, gluing the mirror shells at both ends increases the integration and alignment procedure complexity, not to mention mirror shell instabilities under applied loads, due to the axial constraints. A possible intermediate solution is the use of one stiff spider at one edge, and a thinner spider decoupled in the axial direction by means of flexures on the other side. This solution has already been studied for the EXIST mission[13].
The eXTP mission is now entering phase B. In the following sections, a consolidation of the optical design and a preliminary mechanical design are presented, as a result of a joint collaboration between INAF-Osservatorio Astronomico di Brera, the Chinese Institute of High Energy Physics (IHEP) and Xi'an Institute of Optics and Precision Mechanics (XIOPM).

2. OPTICAL DESIGN

The two types of mirror modules on eXTP, PFA and SFA have the same requirements in term of envelope and effective area. The consequence is that also the optical design can be the same, in order to use the same mandrels for the replication by means of electroforming of the mirror shells. The optical configuration is a classical Wolter-I and the design has been validated with raytracing. In the optimization of the optical design, some parameters are fixed, e.g. the focal length, the t/r ratio, and the total length of the mirror shells. Other parameters have been left free to vary, e.g. the inner and outer diameters, the spacing between the mirror shells and the coating.
As an output, there are a few significant quantities, such as the mass and the effective area at 2 and 6 keV, that are evaluated taking into account the following constraints.[14]

- mass limit: to fit in the overall mass budget, 75-80 kg per module are allocated to the mirror shell mass.
- external and internal envelope.
- the maximum number of mandrels has been limited to 45 for cost and schedule reasons.
- the margin on the effective area at 2 keV and 6 keV must be higher than 10%.
- no on-axis vignetting should be present between two adjacent shells.

Concerning the reflecting coating of the shells, two recipes have been considered, a layer of gold, or gold with carbon overcoating in order to enhance the reflectivity.[15][16] With only the gold coating for all the shells the effective area requirement is well fulfilled at 2 keV, but there is a little margin for 6 keV. The effective area at 6 keV is maximized if a mixed coating is considered, i.e. a bare gold coating for the outer mirror shells and an Au+C bilayer for the inner mirror shells. This effect is visible in Figure 2, where the effective area is shown as a function of the energy, for the two possible coating configurations. The transition radius from one coating to another is approximately mid-way in the series. Experimental tests are currently developed in order to qualify the carbon overcoating properties.

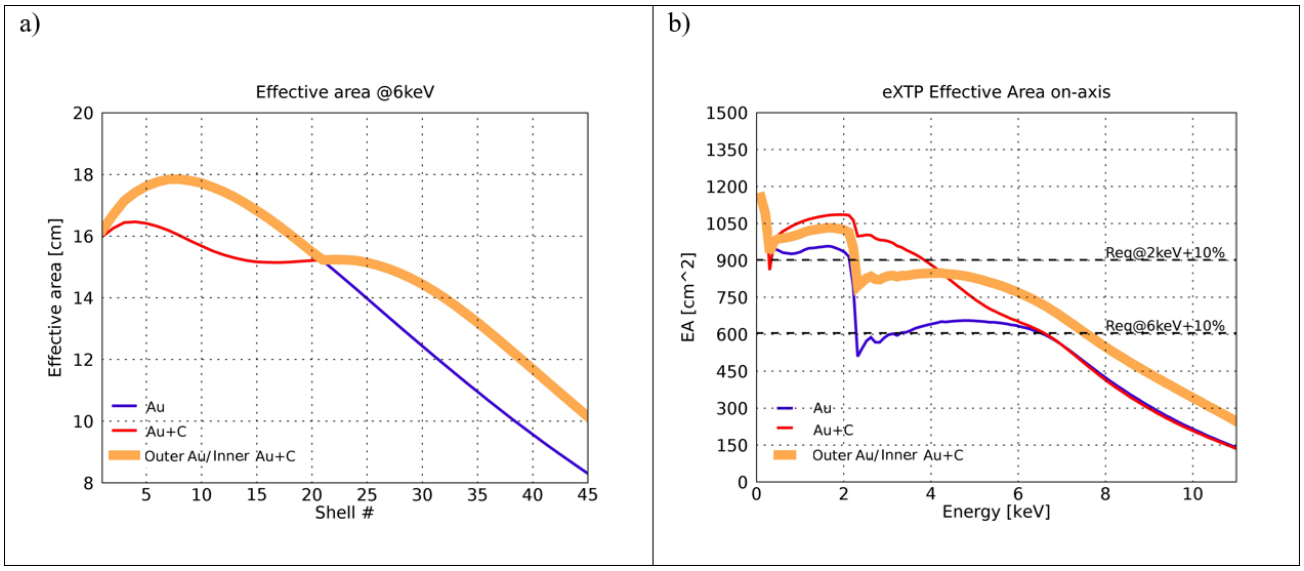

Figure 2 - effective area for each mirror shells (shell n.1 → Φ=474 mm, shell n.45 → Φ=223.4 mm) at 6 keV (a) and the overall effective area as function of the energy (b).

3. MECHANICAL DESIGN

The PFA and SFA have the same optical design and the same constraints in term of effective area and envelope. We also assumed the same mass, the same thickness of the mirror shells, and therefore the same mechanical design. For this reason, they are hereafter referred to as a mirror module (MM). Each MM (Figure 3) comprises:

- *mirror shells*: the optical components, glued to the front spider on the D_{max} side.
- *front spider*: the stiffening structural part connecting the mirror shells by means of 21 spokes. It is made of Inconel 600 alloy.
- *case*: the external titanium tube connecting the spider to the interface flange of the main bench.
- *blocking shell*: the internal blocking tube which limits the stray-light from the innermost shell.

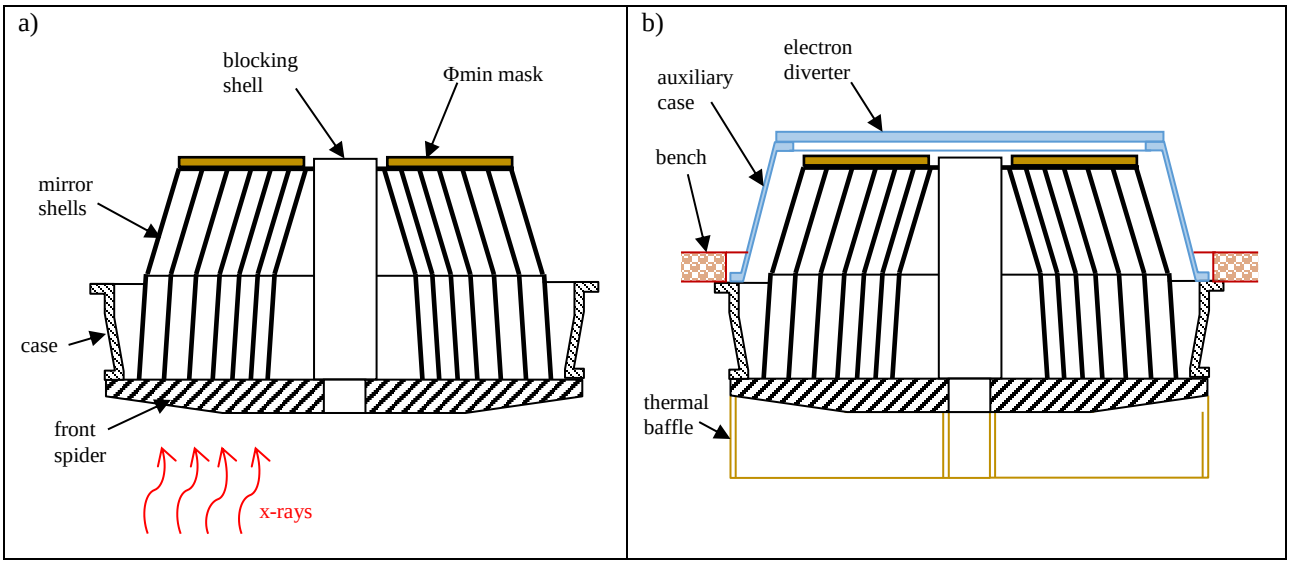

Figure 3 – scheme of the mirror module itself (a) and with its auxiliary items (b).

Other auxiliary items like thermal protections (baffle or filter) and electron diverter will be better defined in the next phase. In this phase, for FEM analysis, the electron diverter is preliminary considered attached to the structure with an auxiliary case made of Aluminium (Figure 4b).

The performed FEM analysis are static (1 g in the three directions, and thermal load), modal, harmonic, and random vibration analysis. These studies allowed us to design a mechanical structure that fulfils the requirements in terms of deformation, strength, stiffness and mass. The requirements and the flight environment are shown in Table 3. The limit for the mass is 100 kg (auxiliary items excluded).

Table 3 – requirements and flight environment used for the FEM analyses.

Static analysis		*Modal analysis*		*Harmonic vibration*		*Random vibration*	
temperature	20±1 °C	direction	freq. [Hz]	Freq. (Hz)	Qualification	Freq. (Hz)	Qualification
axial	7.5 g	axial	> 80	15-35	10.0g	10-150	+3dB/oct
lateral	2 g	lateral	> 40	35-100	3.0g	150-600	$0.05g^2/Hz$
						600-2000	-12dB/oct

In the FEM analysis, not all the 45 mirror shells are modelled, but only 5 shells have been considered: the two innermost shells, the two outermost and one in the middle. The other mirror shells are grouped together in other five mass equivalent components, in order to reduce the number of elements to be modelled. The used FEM software is ANSYS R17.2. The results of the simulations show the critical issue of the glue interface between the mirror shells and the front spider. For this reason, a solution proposed in this paper is the application of a thin mask glued to the rear edges of the mirror shells (Φmin) (Figure 3 and Figure 4a) without any mechanical connection to the other components. The mass of this component is very low (0.2 kg) as it will be made of Titanium. Moreover, it is not expected to obstruct the oncoming X-ray flux as it lies in the shadow of the front spider wheels. This component considerably increases the stiffness. The following FEM results refer to a design with this mask, unless otherwise stated for comparison purposes.

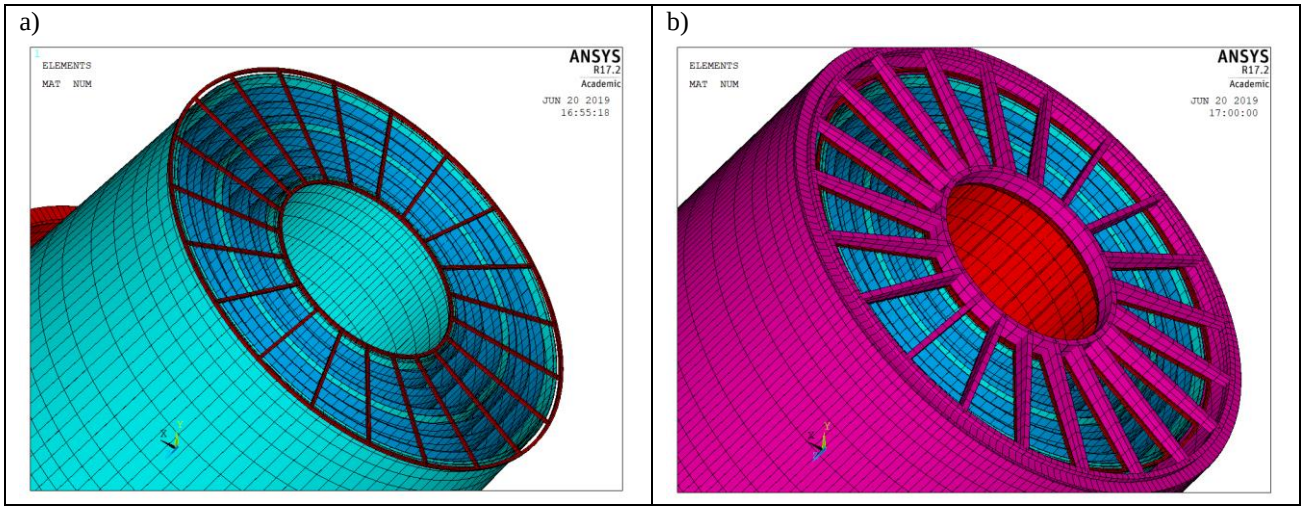

Figure 4 – stiffening mask glued to the Φ_{min} edge of the mirror shells (a) and the simplified model of the electron diverter (b)

3.1 STATIC ANALYSIS

The structural behaviour is linear and the effect can be scaled starting from the case loaded with 1g. This analysis is useful to evaluate the spring back effect during the integration, and the on-ground test campaigns, given the gravity release on-orbit, and to check the survival during the launch. The MM is essentially fixed at three points. The detailed model of this interface will be addressed in a second phase. As for the static analysis, the two extreme and opposite cases of constraints are considered here: the hard-mounted case and the isostatic mount (Figure 5). In the hard-mounted case, the MM is fixed hyper-statically by three couple of bolds that avoid the displacements in all three directions (2x3x3=18 blocked degrees of freedom); in the isostatic case, a single bolt blocks the displacements in three directions, while the other two permit the sliding (3+2+1=6 blocked degrees of freedom).

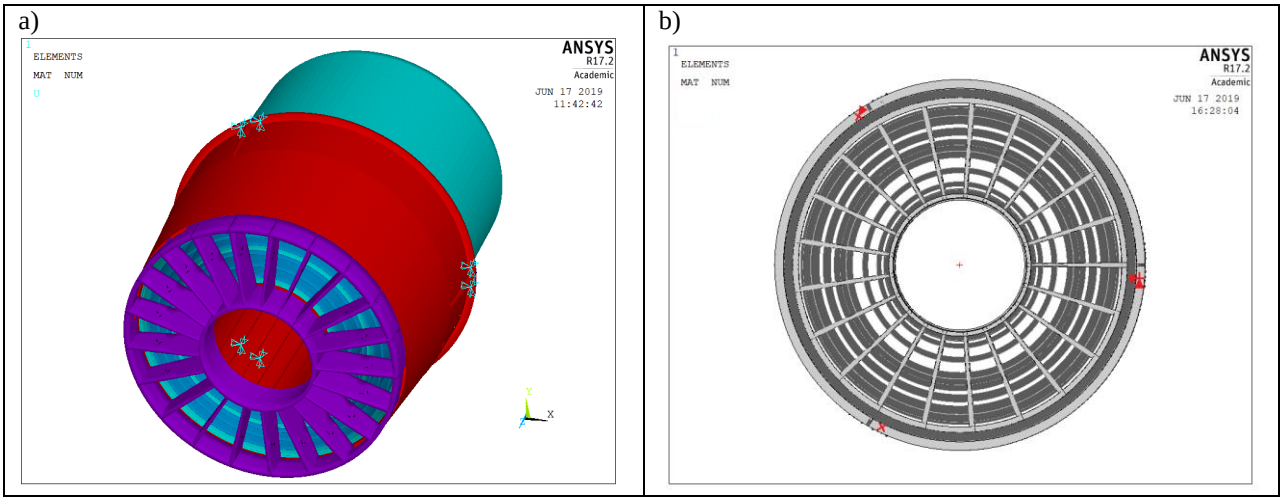

Figure 5 – constraints used in FEM analyses, hard-mounted case (a) and isostatic mount (b)

The used criteria for the survival checking is a comparison between the Von Mises stress scaled from 1 g to the value described in Table 3 with the allowable stress (σ_a) computed according to the formula:

$$\sigma_a = \frac{\sigma_{0.2}}{FS}$$

where the factor of safety (FS) is set to the typical value of '2'. Considering the maximum value of Von Mises stress (σ_{MAX}) for each material as the output of the analysis, the maximum acceptable acceleration (g_{MAX}) is:

$$g_{max} = \frac{\sigma_a}{\sigma_{MAX}}$$

The results are summarized in Table 4 and Table 5. The coordinate system is shown in Figure 5, the axial direction is 'Z' while the XY plane is on the intersection plane between parabola and hyperbola. It has to be noted that the glue is not modelled in this preliminary phase; this assumption is made also for all the other FEM analyses. The results show that the requirements are widely fulfilled. The worst point in the hard-mounting is on the spider and the direction of the acceleration is axial: g_{MAX} is about 60 g w.r.t. the allowable 7.5 g. The stress distribution is shown in Figure 6. In the lateral direction, the margin is larger because the requirement is 2 g.
In the case of isostatic mount, the worst point is still located on the spider, this time in the lateral direction. Also with this constraints the requirements are well satisfied.

Table 4 – result of the static FEM analysis for hard-mount interface

hard-m.		σ_{MAX} [MPa]			g MAX		
	$\sigma_{0.2}$ [MPa]	1g X	1g Y	1g Z	(X)	(Y)	(Z)
Titanium	880	4.59	4.87	3.85	95.9	90.3	114.3
Nickel	400	2.51	2.5	0.51	79.7	80.0	392.2
Inconel600	205	2.98	3.14	1.67	34.4	32.6	61.4

Table 5 - result of the static FEM analysis for isostatic mount

isostatic m.		σ_{MAX} [MPa]			g MAX		
	$\sigma_{0.2}$ [MPa]	1g X	1g Y	1g Z	(X)	(Y)	(Z)
Titanium	880	32.2	16.1	8.1	13.7	27.3	54.3
Nickel	400	10.7	4.67	0.62	18.7	42.8	322.6
Inconel600	205	9.16	6.94	1.71	11.2	14.8	59.9

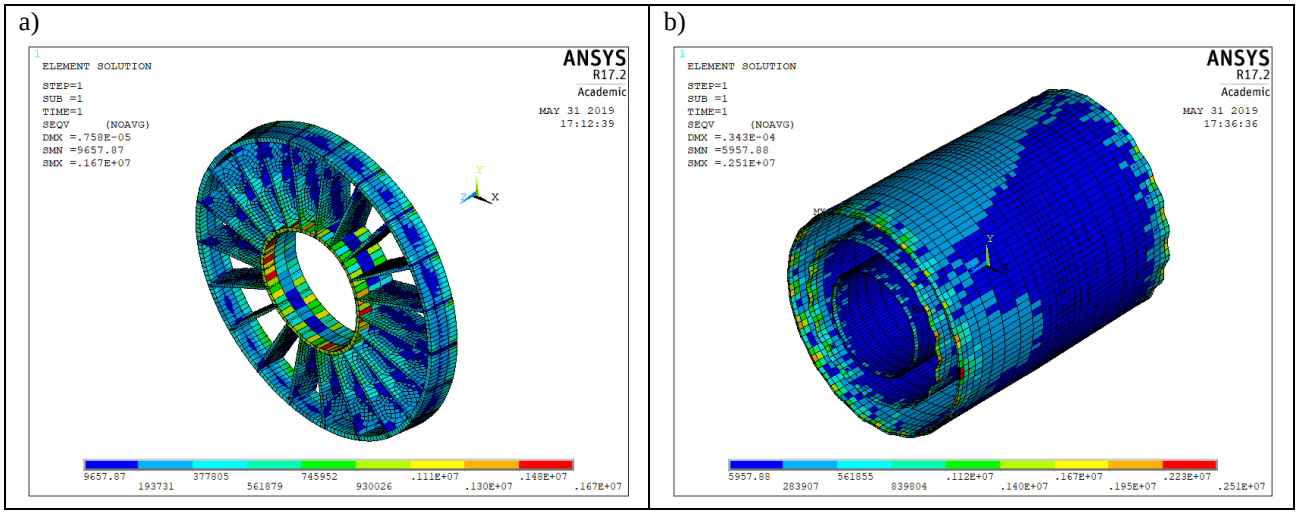

Figure 6 – Von Mises stress [Pa] on the spider for 1 g axial (Z) (a) and on the mirror shells for 1 g lateral (X) (b) in the case of hard-mounted constraints.

The static analysis has been also used to evaluate the thermal effect. Also in this case, the behaviour is linear and the load applied is a temperature difference of 1 °C distributed on all the nodes of the elements. The results are shown on Table 6 for the different constraints. It is clear that, concerning this aspect, the hard-mounting performs worse than the isostatic mount. Anyway, the degradation of the angular resolution is little if the requirement of ΔT of 1°C is considered (Table 3). The HEW (arcsec) in the tables is computed as:

$$HEW = 4 * 206264.8 * \sqrt{2} * rot\theta$$

where 4 is the coefficient from slope to HEW, a factor of √2 take into account the double reflection, 206264.8 is the radians-to-arcseconds conversion factor, $rot\theta$ is the rotation around azimuthal axis in cylindrical coordinates expressed in radians and corresponding to 50% of the reflecting area.

Table 6 – FEM results for a uniform temperature applied (1°C). The HEW_{allow} is set to 5 arcsec, a value that is 33% of total HEW budget for PFA and 8% for SFA.

	hard-mounted			isostatic mount		
	$\sigma_{0.2}$ [MPa]	σ_{MAX} [MPa]	ΔT_{MAX} [°C]	$\sigma_{0.2}$ [MPa]	σ_{MAX} [MPa]	ΔT_{MAX} [°C]
Titanium	880	1.52	289.5	880	0.81	543.2
Nickel	400	0.201	995.0	400	0.164	1219.5
Inconel600	205	0.28	366.1	205	0.256	400.4
	HEW_{allow} [arcsec]	HEW [arcsec]	ΔT_{MAX} [°C]	HEW_{allow} [arcsec]	HEW [arcsec]	ΔT_{MAX} [°C]
Inner shell	5	0.68	7.4	5	0.028	176.8
Mid shell	5	0.79	6.3	5	0.025	196.4
Outer shell	5	0.86	5.8	5	0.037	136.0

The design solution proposed in this paper with use of a mask glued on Φmin side of the shell provide advantages also in term of optical performance. This effect is explained in Figure 7 where on the map of the optical shells the contribution on the HEW is figured out.

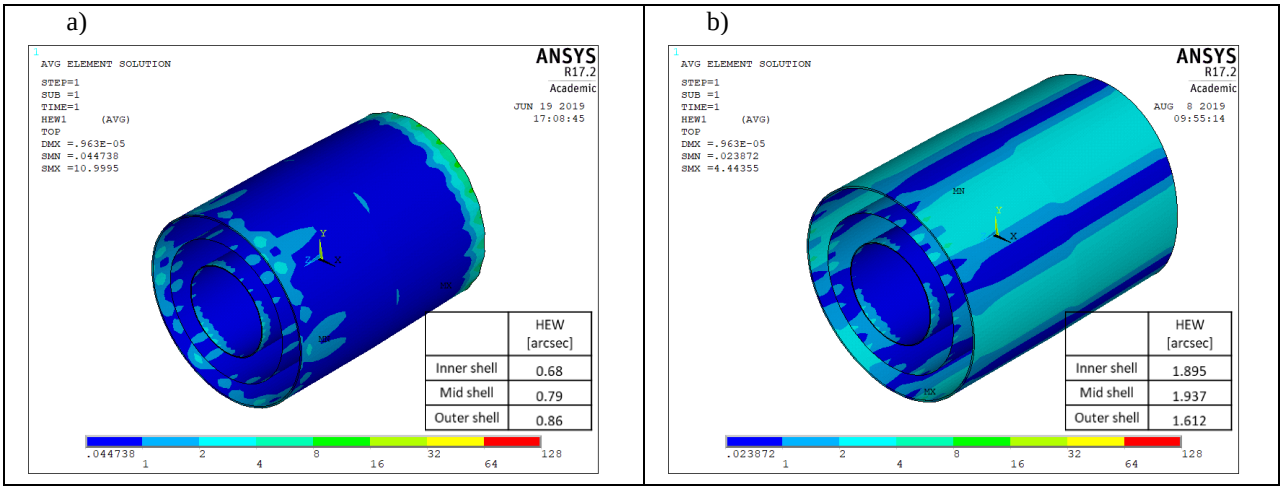

Figure 7 – Optical mirror shells maps: contribution on the angular resolution (HEW, arcsec) due to thermal load (ΔT=1°C, uniform) with the Φ_{min} mask (a) and without the Φ_{min} mask (b) in the case of hard-mounting.

3.2 MODAL ANALYSIS

The modal analysis has been performed to ensure that the minimum natural frequency is not less than 40 Hz in the lateral direction, and 80 Hz in the axial direction. The plot in Figure 8 shows how the natural frequencies are distributed in the spectrum with their participation factor, a parameter indicating the fraction of the mass contributing to the vibration mode (from 0 to 1). For the hard-mounted interface, the first 2 natural frequencies, 76.6 Hz and 117.4 Hz refer to a change in roundness of the mirror shells, 123.8 Hz is the main lateral frequency of the MM and 128.4 Hz is the rotation along the axial direction due to the low thickness of the spider wheels. The main axial natural frequency of the MM is 207.1 Hz. Assuming the isostatic mount, the frequencies decrease, but they remain above the minimum allowed value. Figure 9 shows two representative vibration modes.

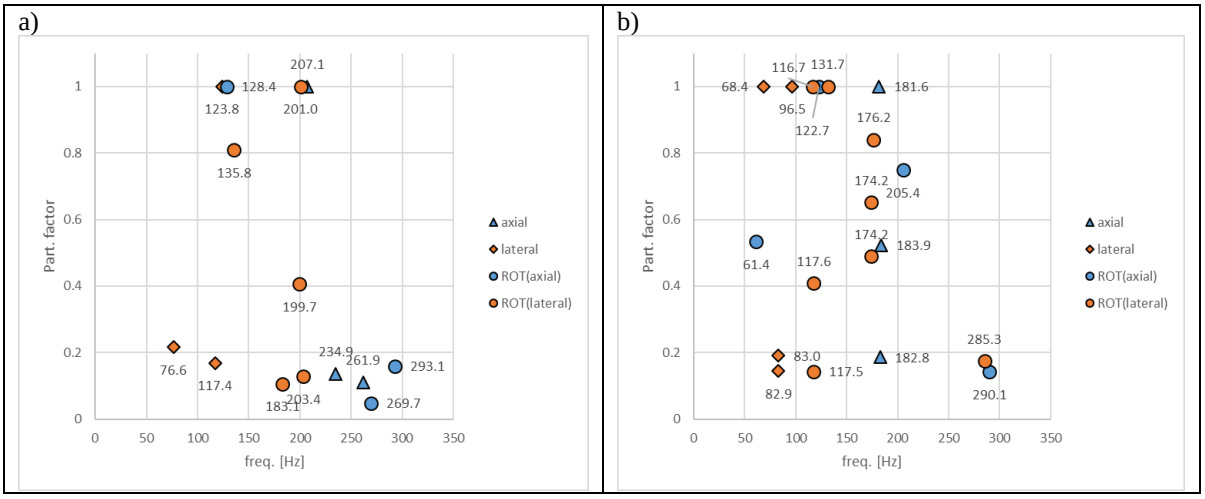

Figure 8 –the modal analysis for hard-mounting case (a) and for the isostatic mount (b). Only frequencies with a participation factor higher than 0.1 are considered.

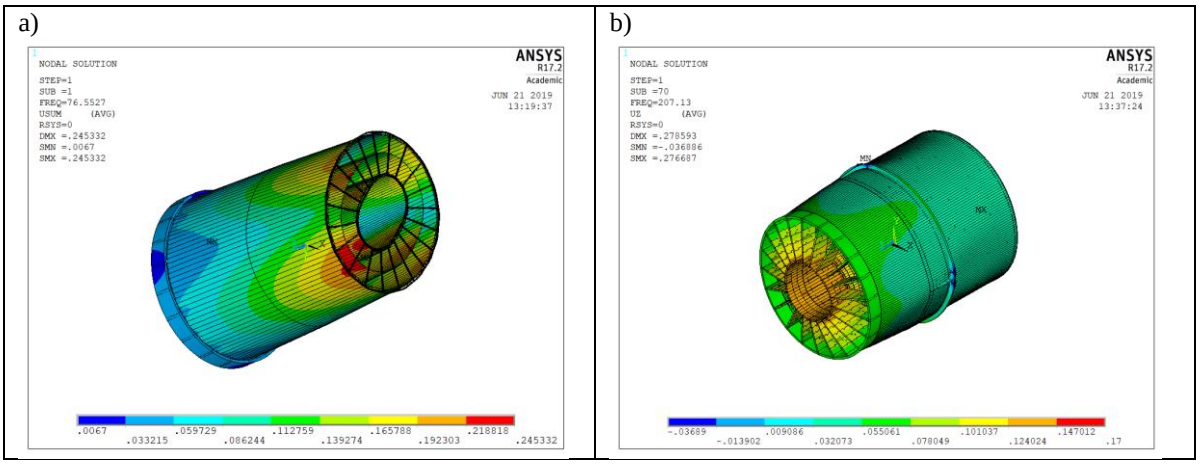

Figure 9 – first vibration modes in the lateral direction at the frequency of 76.5 Hz (the external case is not shown for clarity) (a) and in the axial direction (207 Hz) (b). Both figures refer to the hard-mounting case.

3.3 VIBRATION ANALYSIS

The qualification test on the MM foresees harmonic and random vibrations. In order to optimize the design of the mechanical structure, these analyses have been performed on the FEM. For the harmonic analysis, the output is the stress and the displacements. In Figure 10 the results show the appropriateness of the Φ_{min} mask: at frequencies around 100 Hz, there is an improvement by a four-fold factor.

The random vibration simulation provides statistical values of displacements: they are shown in Table 7 and the behaviour of two representative points is shown on Figure 11 by applying the qualification spectrum of Table 3.

Table 7 – 1σ level of displacements in random vibration simulation

direction	shells [mm]	all [mm]
X	0.603	0.603
Y	0.614	0.614
Z	0.108	0.238

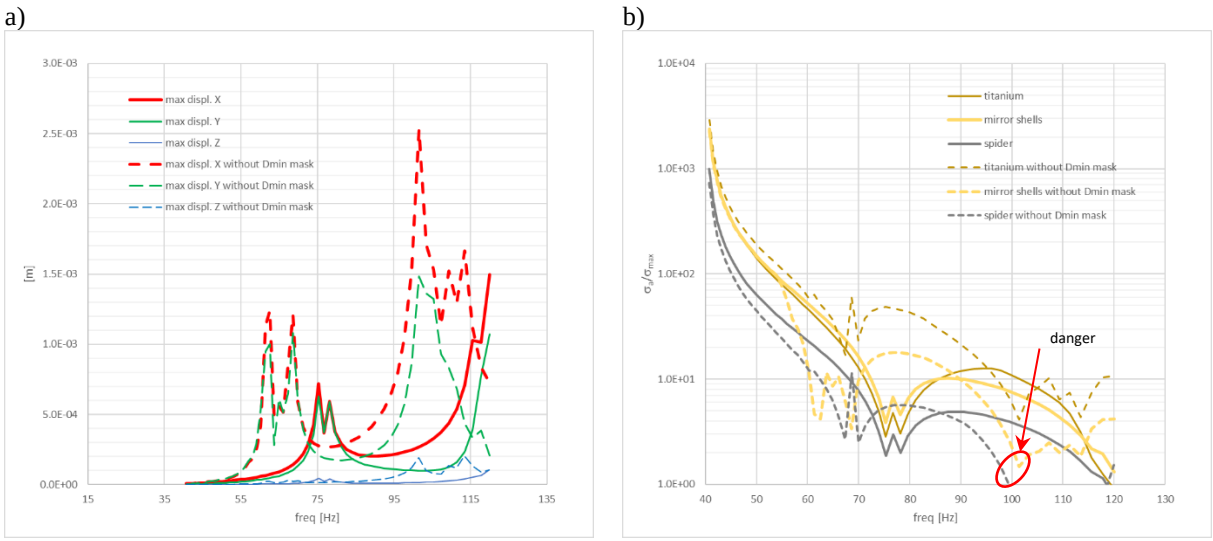

Figure 10 – harmonic analyses considering an amplitude vibration of 3 g along the lateral X direction in the hard-mounted case. Maximum displacements on the mirror shells along the three direction (a) and margin for survival (b): σ_a is the allowable stress as defined in section 3.1 and σ_{max} is the maximum stress identified in the simulation.

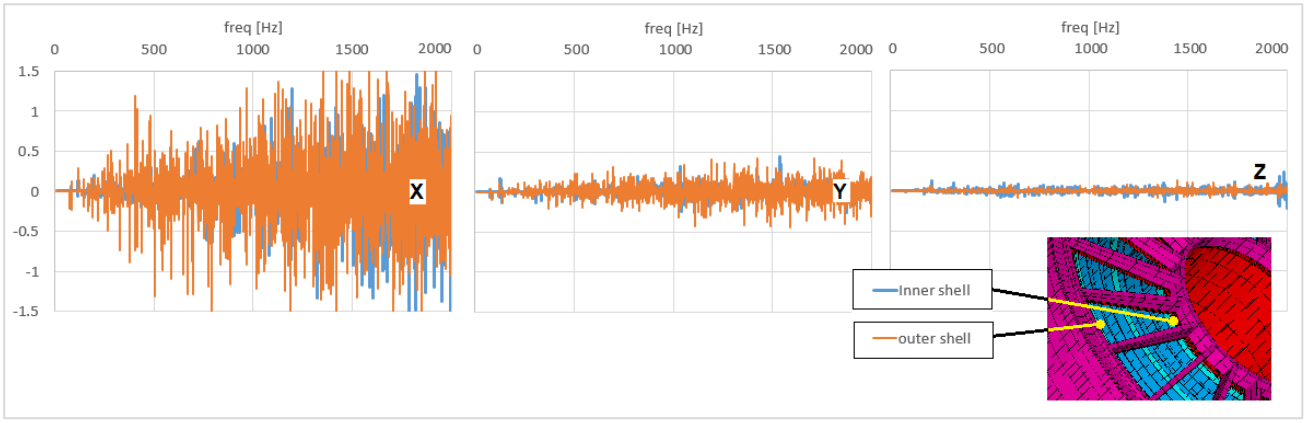

Figure 11 – Vibration of two significant points on the mirror shell, one on the inner shell and one on the outermost mirror shell. The X axis corresponds to the radial direction, Y is the azimuthal direction and Z the axial direction. Amplitude refers to the base excitation.

These vibration analyses demonstrate the need of a system able to blocks the oscillation of the free edge of the thin mirror shell, aiming to avoid mutual collision of the mirror shells. The proposed solution of mask glued at the Φ_{min} edge makes the oscillation more in phase, providing benefit also in term of optical performance, like explained in section 3.1.

4. CONCLUSION

The eXTP mirror modules make use of the fully-qualified technology of electroformed nickel mirror shells. In order to achieve the requirements in terms of effective area and mass, the mirror shells thickness is reduced, close to the limit of what has been realized for current missions or prototypes. Indeed, they are expected to provide an angular resolution in the range of 15-60 arcsec (HEW) in the X-ray energy range of 0.5-10 keV. The mass of the mirror shells is about 75 kg for each module, while the mechanical structure is about 25 kg. A combination of two coatings is proposed to optimize the effective area: Au+C for the inner mirror shells, and a simple Au coating for the outer mirror shells. With this mixed coating, the expected effective area exceeds the minimum required value by 24% at 2 keV and 39% at 6 keV, enough to take into account the spider obscuration (~10%), the possible thermal filter absorption (few percent), the loss of efficiency due to manufacturing or alignment issues. The critical point that will be further analysed and tested in the next phases is the connection between the mirror shells and the spider wheels, where the stresses reach very high values. The relative

long length (600 mm) of the mirror shells compared to the thickness leads to problems connected to the vibration during the launch phase. To solve this problem, we propose to use a mask glued to the Φ_{min} end of the shells to damp the vibrations, leaving the axial expansion free between the mirror shells and the mechanical structure.
The mission is currently at the beginning of the phase B. In Italy and China some preliminary tests have been developed, and other prototypes will be assembled in the near future in order to fully demonstrate the feasibility.

ACKNOWLEDGMENT

This research is supported for the Italian part by ASI with ASI/INAF contract n. 2018-19.HH.0.

REFERENCES

[1] S. N. Zhang, M. Feroci, A. Santangelo, et al., "eXTP: Enhanced X-ray Timing and Polarization mission", Proc. SPIE. 9905, 99051Q. (2016) doi: 10.1117/12.2232034
[2] Pareschi, G., Attina', P., Basso, S., Borghi, G., Burkert, W., Buzzi, R., Citterio, O., et al., "Design and development of the SIMBOL-X hard x-ray optics", Proc. SPIE 7011, 70110N (2008)
[3] Pareschi, G., Tagliaferri, G., Attinà, P., Basso, S., Borghi, G., Citterio, O., Civitani, M., Cotroneo, V., Negri, B., Sironi, G., Spiga, D., Vernani, D., Valsecchi, G., "Design and development of the optics system for the NHXM hard X-ray and polarimetric mission", Proc. SPIE 7437, 743704 (2009)
[4] Basso, S., Pareschi, G., Tagliaferri, G., Attinà, P., Borghi, G., Citterio, O., Civitani, M., Cotroneo, V., Negri, B., Sironi, G., Spiga, D., Vernani, D., Valsecchi, G.,"The optics system of the New Hard X-ray Mission: design and development", Proc. SPIE 7732, 7732-43e (2010)
[5] Tkachenko, A., Pavlinsky, M., Levin, V., Akimov, V., Krivchenko, A., Rotin, A., Kuznetsova, M., Lapshov, I., Yaskovich, A., Oleinikov, V., Gubarev, M., Ramsey, B., "ART-XC/SRG: joint calibration of mirror modules and x-ray detectors", Proc. SPIE 10397, 103971J (2017); doi: 10.1117/12.2272710
[6] Weisskopf, M. C., Ramsey, B., O'Dell, S., Tennant, A., Elsner, R., Soffitta, P., Bellazzini, R., Costa, E., Kolodziejczak, J., Kaspi, V., Muleri, F., Marshall, H., Matt, G., Romani, R., "The Imaging X-ray Polarimetry Explorer (IXPE)", Proc. SPIE 9905, 990517 (2016); doi: 10.1117/12.2235240
[7] Citterio, O., Bonelli, G., Conti, G., Mattaini, E., Santambrogio, E., et al., "Optics for the x -ray imaging concentrators aboard the x -ray astronomy satellite SAX", Proc. SPIE 0830, (1988); doi: 10.1117/12.942174
[8] Wells, A., Owens, A., Sims, M., "X-ray imaging and spectroscopic performance of the JET-X telescope on the Spectrum X-Gamma", Proc. SPIE 2279, (1994); doi: 10.1117/12.193166
[9] Gondoin, P., Aschenbach, B., Beijersbergen, M., Egger, R., Jansen, F., Stockman, Y., Tock, J., "Calibration of the first XMM flight mirror module: I. Image quality", Proc. SPIE 3444, (1998); doi: 10.1117/12.331243
[10] Arcangeli, L., Borghi, G., Bräuninger, H., Citterio, O., et al., "The eROSITA X-ray mirrors: technology and qualification aspects of the production of mandrels, shells and mirror modules", Proc. SPIE 10565, 1056558 (2010); doi: 10.1117/12.2309182
[11] Ramsey, B., "Optics for the imaging x-ray polarimetry explorer", Proc. SPIE 10399, 1039907 (2017); doi: 10.1117/12.2275502
[12] Basso, S., Citterio, O., Pareschi, G., Spiga, D., Tagliaferri, G., et al., "The optics system of the New Hard X-ray Mission: status report", Proc. SPIE 8147, 814709 (2011); doi: 10.1117/12.895324
[13] Basso, S., Tagliaferri, G., Natalucci, L., Parodi, G., Villa, G., Bazzano, A., Caraveo, A., Conconi, P., et al., "The X-ray mirrors for the EXIST/SXI telescope", Proc. SPIE 7732, 77324C (2010); doi: 10.1117/12.857308
[14] Spiga, D., Tagliaferri, G., Pareschi, G., Feroci, M., Santangelo, A., "Specifications for the enhanced X-ray Timing Polarimeter (eXTP)", INAF/OAB technical report 01/2017 (2017)
[15] Pareschi, G., Cotroneo, V., Spiga, D., Barbera, M., Artale, M. A., Collura, A., et al., "Astronomical soft X-ray mirrors reflectivity enhancement by multilayer coatings with carbon overcoating," Proc. SPIE 5488, 481 (2004)
[16] Cotroneo, V., Spiga, D., Barbera, M., Bruni, R.J., Chen, K., Marcelli, A., et al., "Carbon overcoatings for soft X-ray reflectivity enhancement", Proc. SPIE 6688, 66880U (2007)
[17] Pareschi, G., Civitani, M. M., Sironi, G., Yang, Y., Valsecchi, G., Magagnin, L., "Reflectivity-enhancement at low x-ray energies in astronomical telescopes using low-density overcoatings: alternative materials and deposition methods", Proc. SPIE this conference (2019)